COBEM 2021 Florianópolis - Brasil
26th ABCM International Congress of Mechanical Engineering
November 22-26, 2021. Florianópolis, SC, Brazil

COB-2021-0891
STATIC EQUILIBRIUM ANALYSIS OF A DISTRIBUTION LINE RIDING ROBOT WITH PASSIVE BALANCING SYSTEM

João Vitor Fernandes de Brito
Estevan Hideki Murai
Gustavo Queiroz Fernandes
Rogério Augusto Antunes Pereira
Daniel Martins
Federal University of Santa Catarina. Campus Universitário Reitor João David Ferreira Lima, s/nº - Trindade, Florianópolis – SC, 88040-900
joaov.brito92@gmail.com
estevan.murai@ufsc.br
gustavo.fernandes@posgrad.ufsc.br
rogerio.antunes@posgrad.ufsc.br
daniel.martins@ufsc.br

Roberto Kinceler
Alessandro Pedro Dadam
Centrais Elétricas de Santa Catarina S.A. Av. Itamarati, 160 - Itacorubi, Florianópolis - SC, 88034-900
rkinceler@celesc.com.br
alessandropd@celesc.com.br

Abstract. *Brazil presents an extensive distribution grid. Power lines age and they need constant maintenance to keep a distribution grid reliable. However, given the Brazilian distribution grid extension, performing regular inspections in distribution lines is a challenge. One approach is to automate the inspection using robots. When developing an inspection robot for distribution lines, a key issue is designing a robot that is capable of transposing several different obstacles and that has a low mass. Besides that, when the robot is operating in the distribution line it has to remain stable. In this paper, the static equilibrium analysis of a distribution line riding robot with passive balancing system is done. Initially, the geometries of the distribution line components, such as insulators and cross arms, are presented. The distribution line riding robot is also presented, along with its geometric properties and mass distribution. The static equilibrium equations are developed and implemented in Matlab. The robot wheel geometry is considered along with the insulators geometry, analyzing whether the robot is stable or unstable for a given robot position. Finally, it is devised a stability map that allows the designer to compare the stability of different wheel geometries.*

Keywords: *static equilibrium analysis, distribution line inspection robot, passive balancing system, robot stability analysis.*

1. INTRODUCTION

Overhead distribution lines correspond to more than 95% of the Brazilian medium-voltage power supply grid. At the same time, aged components and elements that are badly installed, missing or broken may lead to the inefficiency, or even to the complete interruption in the power supply. Pollution and strong weather conditions, such as wind and snow, may also accelerate corrosion and other degradation effects, causing faster aging of the distribution line components (Prates *et al.*, 2019). This inefficient energy provision represents both financial losses and life risk conditions for citizens, once health, sanitation, transportation and other systems rely on energy to work. Just for the purpose of comparison, according to Jenssen *et al.* (2018), a power supply interruption of half an hour in the USA leads to $15,709 loss only for medium and large industries. Therefore, although Brazil presents an extensive distribution grid, electrical utility companies have to efficiently provide both preventive and corrective maintenance along the whole power lines.

The current solution found by most of the energy providers is to allocate and train professionals to perform visual inspection through walking patrols. On the other hand, human inspections are prone to misinterpretations and incorrect diagnosis, sometimes leading to inappropriate maintenance actions (Prates *et al.*, 2019). In order to make the inspection process faster, drones and other unmanned aerial vehicles (UAVs) may also be applied at some conditions. However,

once most of the distribution lines are located in urban areas, local regulations impose limits in regard to size, weight and minimum distance from people and buildings that UAVs may reach, making the use of UAVs unfeasible to distribution line inspection in a general perspective. As a solution, electrical utility companies have attempted to automate the inspection processes through the use of robots that can ride along the distribution lines. Some of the robots found in the literature are described in Sec. 2.

The development of a distribution line inspection robot is a complex task due to the variability of elements present on the energy grid, such as insulators, overhead switches, fuse-cutouts, cross arms and even Rufous Hornero nests, that may act as obstacles for the robot. Most of the solutions available in the literature approach this challenge by adding more degrees of freedom to the robot, allowing it to avoid or contour the obstacles when necessary. However, more degrees of freedom means a higher number of parts and actuators, increasing both the robot mass and volume. Mass is an important design requirement because the robot cannot exceed the distribution line load capacity, specially the aluminium conductors load capacity. A higher mass may also mean a higher power consumption and more battery cells. Besides that, volume is also an important design constraint as the robot may contact different points in the distribution line at the same time. Depending on the materials used, this double contact may cause short circuits and consequent accidents. In addition, extra degrees of freedom may also demand more reliable electronics and control systems in order to maintain the robot stable. Besides that, more components increases the robot cost, which is an important characteristic to guarantee the economic feasibility of using a robot to inspect distribution lines.

Considering the points exposed above, “Centrais Elétricas de Santa Catarina” (Celesc), in partnership with the Laboratory of Applied Robotics (LAR) from the Federal University of Santa Catarina (UFSC) are developing a robot that can roll over distribution lines obstacles. For the robotic system under development to fulfill its function, it needs to be able to move through the distribution grid effectively and efficiently. Thus, the robotic system needs to be robust and secured to the distribution line. Due to the direct contact to obstacles and the consequent disturbances that may arise from it, the robot designing also includes the determination of the surface geometry that interacts with the distribution line components. A proper surface geometry, associated with a low center of mass, allows the robot to return to an equilibrium condition when any disturbance occurs.

This paper assesses the static equilibrium capability of three robot wheel geometries. Stability maps are produced for each analyzed scenario, relating different contact points along the wheel to a maximum stability inclination angle. Section 2 carries out a brief review on what can be found in the literature in regard to distribution lines inspection robots. Section 3 describes the geometrical characteristics of the robot wheels considered in this study. Section 4 presents the theory and mathematical formulation required for the static stability analysis. The results are discussed in Section 5 whereas a summary of the conclusions is given in Section 6.

2. ON THE DESIGN OF INSPECTION ROBOTS FOR TRANSMISSION AND DISTRIBUTION LINES

This section presents a brief review on distribution lines inspection robot. By reviewing these robots, it is expected to show different approaches used for obstacle transposing and how they affect the robot in the overall usage.

Initially, a search for distribution lines inspection robots was carried out. Some robots for transmission line inspection can be seen in Katrasnik *et al.* (2010); Miller *et al.* (2017); Jalal *et al.* (2013); Toussaint *et al.* (2009); Aracil *et al.* (2002); Hydro-Québec (2018); IEEE (2010); Rodmilans *et al.* (2010); Fan *et al.* (2011); Zongyuan *et al.* (2010); Wang *et al.* (2010); Parker and Draper (1998); Gonçalves and Carvalho (2014). However, no inspection robot for distribution lines was found that satisfied the project requirements. The search was broaden to robots for both distribution and transmission lines.

Three concepts stood out as frequently used approaches to inspect distribution or transmission lines. These three concepts are classified here in three categories:

Category A (Cat.A): robots in this category present a heavy and movable trunk. The robot transposes obstacles by moving the trunk, which maneuvers the robot center of mass (CM). Figure 1a shows a representative example of Cat.A robots.

Category B (Cat.B): robots in this category are similar to robots in Cat.A, but they have an additional degree of freedom at their supporting arms. The additional degree of freedom allows the robot wheel to move laterally. Figure 1b shows a representative example of Cat.B robots.

Category C (Cat.C): robots in this category have three robotic arms, each arm with 2 degrees of freedom. Figure 1c shows a representative example of Cat.C robots.

Robots in Cat.A change the CM position, which results in the robot taking off one wheel from the line. The robot moves forward, passing the front wheel over the obstacle. The procedure is repeated to move the back wheel over the obstacle. Cat.A robots make use of at least one motor for each wheel and one servomotor to control the trunk position. Besides that, Cat.A robots also have two arms with one wheel each, a beam connecting the arms and serving as a linear

rail. Although simple, this concept present its limitations. For instance, when climbing hills, the front wheel needs to be lifted high above the power line. Thus a longer line rail is needed, extending both line rail ends. However, a longer line rail being tilted up and down close to the power line, cross arm and poles may result in undesired short circuits.

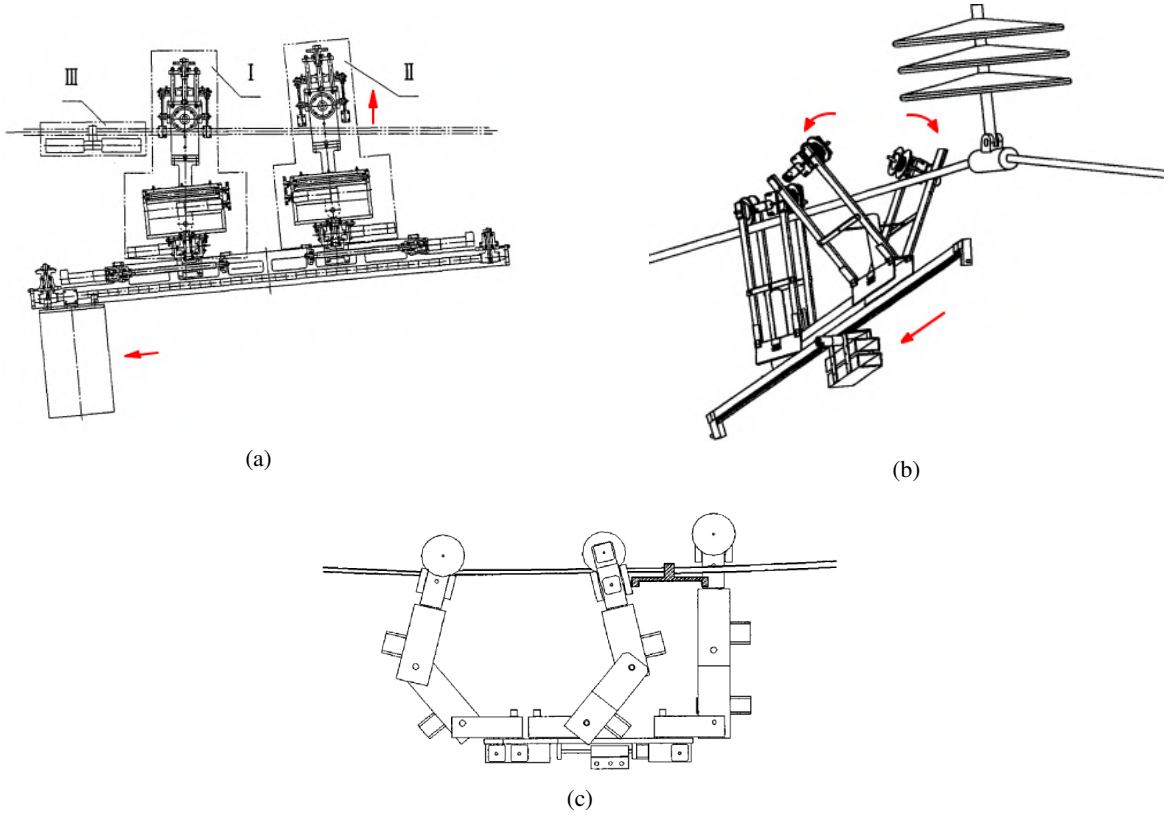

(a) (b) (c)

Figure 1: The three most common approaches for transposing obstacles in transmission lines: (a) category A. Adapted from Fan *et al.* (2011). (b) Category B. Adapted from Rodmilans *et al.* (2010). (c) Category C. Adapted from Zongyuan *et al.* (2010).

Similarly to Cat.A robots, robots in Cat.B move the heavy trunk to maneuver the robot CM. By moving the robot CM, the wheel is risen at enough height so that the wheel is no longer in contact with the cable. Then, the wheel is moved laterally by means of rotation or translation. From this point, the transposition proceeds as in the robots in Cat.A. In relation to robots in Cat.A, robots in Cat.B have a shorter line rail but they present more motors and movable parts. Thus, robots in Cat.B tend to be a more complex and heavier than robots in Cat.A.

Cat.C robots transpose obstacles by moving one arm over the obstacle at a time. This concept requires more movable parts and motors than robots in Cat.A and Cat.B.

A qualitative analysis indicated that Cat.A robots are the lightest robots among the robots exposed in Fig. 1. Therefore, it was considered the most promising concept to be adapted to distribution lines. However, after it was scaled down to distribution lines application, a Cat.A robot would require a large volume during transpositions. Besides that, the robot could only be used in the cable near the cross arm extremity and the robot mass would be close to the design limit.

A robot for distribution line inspection presents different design requirements than a robot for transmission line inspection. Transmission lines usually uses aluminum conductor steel-reinforced (ACSR) cables, which present a higher mechanical strength than the equivalent all aluminum conductor (AAC), commonly used in distribution lines (Celesc, 2015). Thus, a robot for inspecting distribution lines needs to be significantly lighter then a robot to inspect transmission lines.

Besides the lightweight requirement, in a distribution line the obstacles are more diverse, including human intervention. The distances between poles are shorter, resulting in more obstacles per meter travelled along the line. Therefore, there are more transposition maneuvers per meter inspected and it is desired a highly efficient transposition operation. When analysing Cat.A robots, it is noticed that their obstacle transposition approach must be done carefully, controlling the robot CM in order to balance the robot over the cable at a single contact point while also moving the robot forward. This obstacle transposition approach can be time consuming.

In transmission lines, the cable is usually hanged at the bottom of insulators (see Fig. 1b), which means the majority of the obstacle to be transposed is above the cable. The obstacle-free path is below the cable, and designing a robot to

move below the cable yields a naturally stable robot. As Fig. 1 shows, the robots center of mass are below the cable.

On the other hand, in distribution lines the cable passes over the insulators. Thus, the obstacles to be transposed are below the cable. The obstacle-free path is above the cable, and designing a robot to transpose obstacles moving above the cable yields a naturally unstable robot.

A promising transposition principle found in the survey was running over the obstacles. In this principle, the robot wheel is carefully designed so that the robot can run over the obstacles and remain relatively stable and secured to the power line. One example of a wheel capable of running over obstacle can be seen in the transmission line inspection robot LineRanger (Hydro-Québec, 2018), developed by Hydro-Québec. Hibot Expliner (IEEE, 2010) uses the run over strategy for small obstacles and Cat.B approach for transposing larger obstacles.

Therefore, a new concept was designed using the running over obstacle strategy. The robot is designed to be light weight, compact and with few movable parts. The robot is presented in Section 3. However, stability when transposing obstacles is a critical point in this design. Thus, an equilibrium analysis is required. Section 4 presents the static equilibrium tool developed to analyze the robot stability when transposing obstacle.

3. GEOMETRICAL CHARACTERISTICS

The robot design consists of a wheel, which rotates as it moves along the cable, and a suspended outer structure that holds actuators, sensors, batteries and other electronic devices. The robot mass is distributed in a manner that the wheel is made as light as possible, while the outer structures hold heavy components. As the outer structure is positioned in the robot lower part, the robot CM is located below the contact point between the robot wheel and the distribution line, increasing the robot stability.

There are two critical steps during transposition: climbing over the obstacles and stepping down from the obstacles to the cable. The wheel geometry must provide stability when climbing several types of insulators. Thus, the wheel geometry must match the insulators profile. On the other hand, when stepping down from insulator to the cable, the wheel must present a geometry that compensates some misalignment. Thus, even when the center part of the wheel is not aligned to the cable, the wheel geometry should self-align the robot to the cable. At last, the wheel radius should be small so that it keeps the robot low over insulators and on the cable, maintaining the center of mass below the contact point between the robot and the distribution line.

As shown in Fig. 2, three different wheel geometries are compared in terms of stability. The first one (Fig. 2a) has two arcs with opposing concavities. The second wheel (Fig. 2b) is completely convex. The third concept (Fig. 2c) has a fully concave profile.

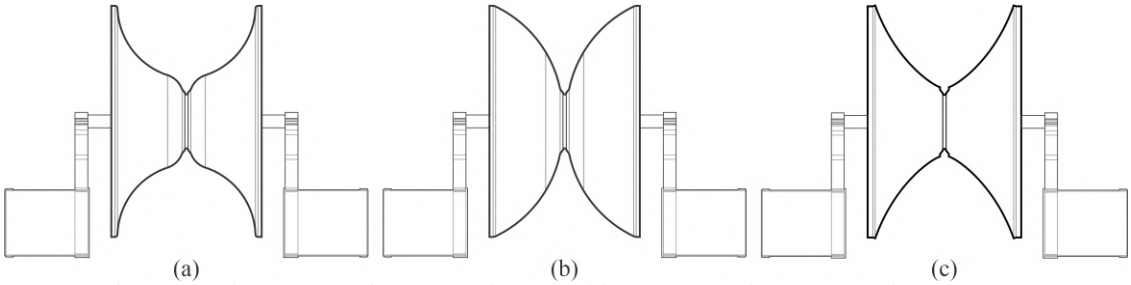

Figure 2: Wheel geometries assessed: (a) double curvature, (b) convex and (c) concave.

Prior to the equilibrium analysis, it is necessary to establish some geometrical characteristics: the initial rotation point (RP), center of mass (CM) and angular displacement applied to the robot (α). To compare the wheel geometries, all three robots in Fig. 2 are assumed to have the same center of mass, with a total robot mass of 15 kg. Additionally, the same rotation points are analyzed for the three wheels. Therefore, the geometrical characteristics discussed in this section are valid for the three concepts.

The initial points coordinates are defined in the Cartesian system presented in Fig. 3. This Cartesian system is centered on the point of contact between the cable and the wheel center channel. The x axis is parallel to the wheel axis, which is horizontal in the initial position analysis, and oriented to the right. The y axis is perpendicular to the wheel axis and oriented upward. For this analysis, it is considered that the robotic system is symmetric, with the center of mass located over the y axis.

The angular displacement is defined by the angle between an horizontal line passing through the updated Cartesian center and the updated axis of the wheel, see Fig. 4. For the equilibrium analysis, it is considered that the contact between the wheel and the insulator is limited or in the verge of being limited to a single point, the rotation point, due a clockwise angular displacement applied to the robotic system.

A distribution line presents different types of insulators, such as pin-type and line post (Celesc, 2014). However, in general the insulators top part present similar dimensions and geometry, see Fig. 5. The top part diameter is approximately

125 mm. Based on the insulators geometry; on the consideration that the contact between the wheel and insulator is on the verge of being limited to a single point; and on the application of a clockwise angular displacement, a feasible region for the rotation point was established, Fig. 5c. When the insulator is centralized in relation to the wheel, the rotation point is furthest to the right, at 62.5 mm from the center. Then, it is considered that the rotation point shifts to the left up to 80 mm, keeping a clockwise rotation. The central region is disregarded because the insulator cannot reach it. The same feasible region was used in the three wheel curvatures evaluated, always considering a clockwise angular displacement for the robotic system.

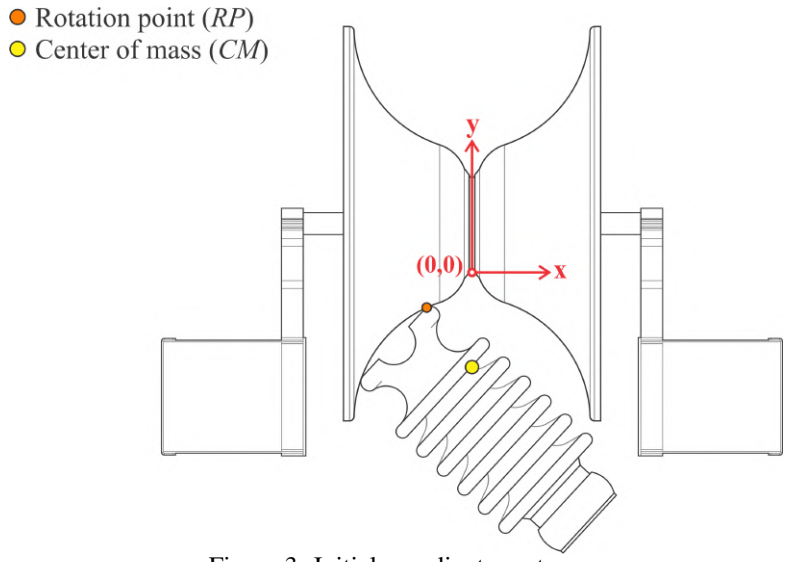

Figure 3: Initial coordinate system.

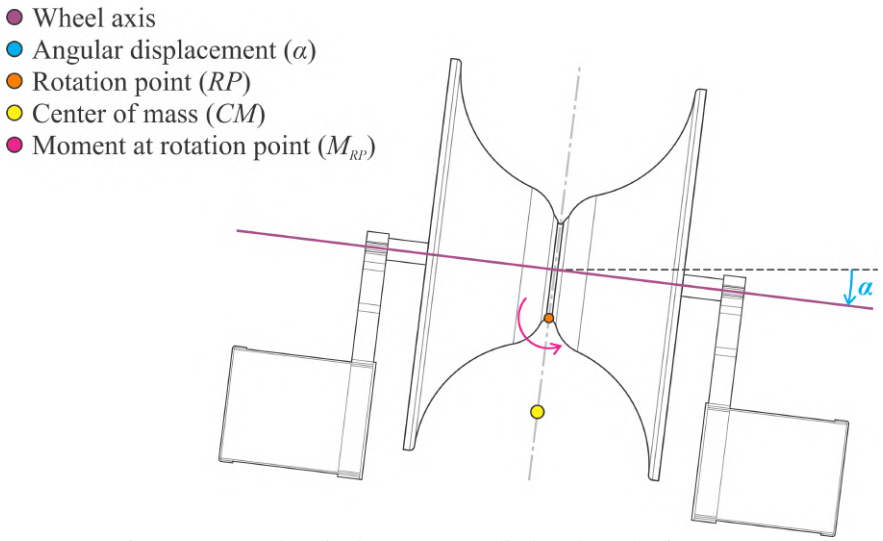

Figure 4: Angular displacement applied to the robotic system.

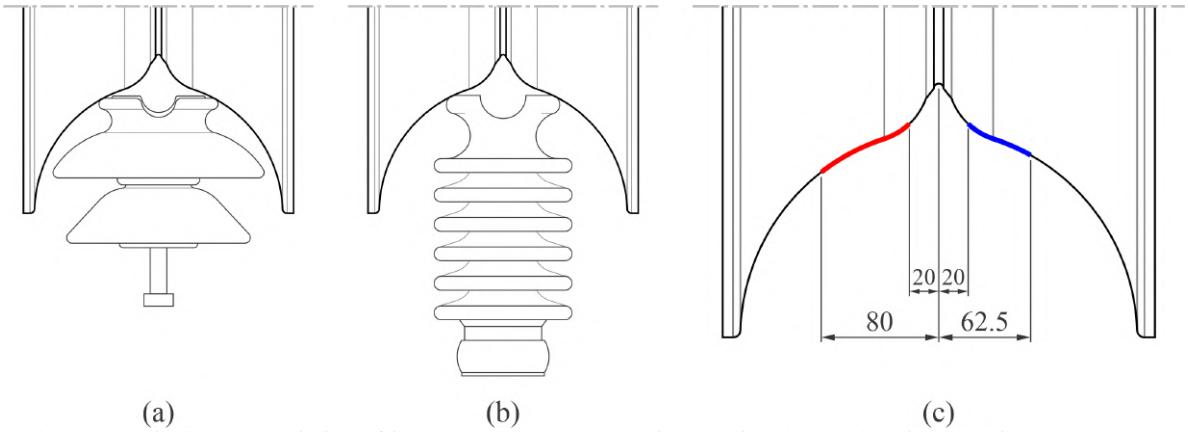

Figure 5: Geometrical characteristics of insulators top part: (a) pin-type insulator. (b) Line post insulator. (c) Feasible region for the rotation point.

4. STATIC EQUILIBRIUM ANALYSIS

This analysis consists on the frontal evaluation of the moment applied to the robot due to its own weight around a rotation point and angular displacement applied to the robot. In order to calculate this moment, first it is necessary to define the relative position vector from the rotation point to the robot center of mass.

The geometric characteristics presented in Section 3 provide the angular displacement applied to the robot, the center of mass initial position ($\mathbf{CM}$) and rotation point ($\mathbf{RP}$). With these variables, it is possible to define the center of mass updated position and the rotation point updated position, Eq. 1 and 2. The relative position vector ($\mathbf{L}$) is obtained by vector subtraction of these updated positions, Eq. 3.

$$\mathbf{CM}' = \left[|\mathbf{CM}|.cos\left(atg\left(\frac{CM_x}{CM_y} \right) - \alpha \right), |\mathbf{CM}|.sin\left(atg\left(\frac{CM_x}{CM_y} \right) - \alpha \right), 0 \right] \tag{1}$$

$$\mathbf{RP}' = \left[|\mathbf{RP}|.cos\left(atg\left(\frac{RP_x}{RP_y} \right) - \alpha \right), |\mathbf{RP}|.sin\left(atg\left(\frac{RP_x}{RP_y} \right) - \alpha \right), 0 \right] \tag{2}$$

$$\mathbf{L} = [L_x, L_y, 0] = \mathbf{CM}' - \mathbf{RP}' \tag{3}$$

The moment around the rotation point ($\mathbf{M_{RP}}$) is defined by the cross product of the relative position vector and the weight vector (Hibbeler, 2017). The adopted coordinated system for this analysis grants that the weight vector is a vector parallel to the y axis (Fig. 6). Therefore the cross product results in Eq. 4.

$$M_{RPz} = -|\mathbf{W}|.L_x \tag{4}$$

A Matlab script was developed in order to evaluate the capability of the robotic system to passively achieve equilibrium for a set of distinct rotation points and initial angular displacements. The inputs for this script are listed below.

- Set of coordinates of points on the wheel curvature (Fig. 7).
- Upper and lower boundaries for the horizontal coordinate of the rotation point.
- Mass and mass center coordinates of the robotic system.
- Range of angular displacement applied to the system.

The script developed was initially used to evaluate the capability to achieve passive equilibrium with distinct wheel curvatures, Fig. 2. Later, it was used to evaluate the impact of modifying the center of mass of the robotic system on its capability of achieving passive equilibrium. Some of these results are presented in the following section.

5. RESULTS AND DISCUSSIONS

The output of the developed script is a three-dimensional graph in which the first axis is the moment ($\mathbf{M}_{RP}$), the second axis is the applied angular displacement (α) and the third axis is the initial horizontal coordinate of the rotation point (RP_x), Fig. 8. The graphs take the shape of a three-dimensional surface. To facilitate the interpretation and comparison, the results are presented in a two-dimensional view with a color scheme to identify the value of the moment

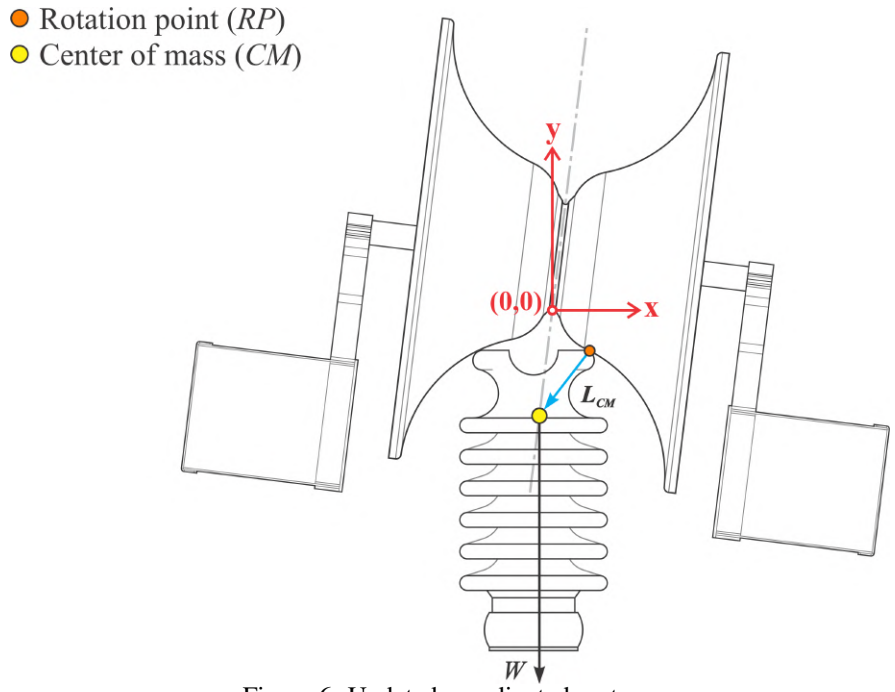

Figure 6: Updated coordinated system.

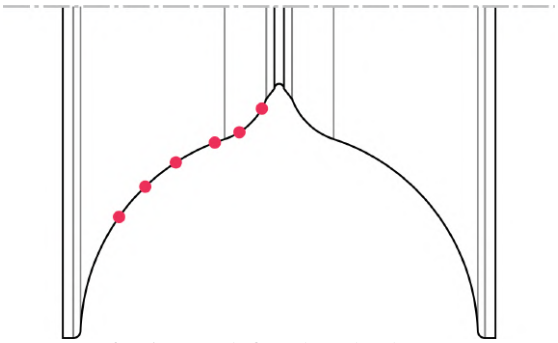

Figure 7: Set of points to define the wheel curvature equation.

($\mathbf{M}_{RP}$), see Fig. 9 to 11. The transition between cyan and yellow indicates configurations which the moment ($\mathbf{M}_{RP}$) will be close to zero, thus the robotic system may maintain the current applied angular displacement (close to stability). The dark red color represents a configuration which the moment ($\mathbf{M}_{RP}$) will be negative, which will tend to increase the clockwise angular displacement, therefore further decreasing the moment ($\mathbf{M}_{RP}$)(unstable). The dark blue color indicates a configuration which the moment ($\mathbf{M}_{RP}$) will be positive, which will tend to reduce the clockwise angular displacement, therefore decreasing the moment ($\mathbf{M}_{RP}$) approaching stability.

Studying the equations that are used to determine the moment ($\mathbf{M}_{RP}$), it was expected the moment magnitude to increase with the increase of the vertical position of the rotation point (RP_y) and decrease of the vertical position of the center of mass (CM_y). This behaviour can be seen through Fig. 9, 10 and 11. The wheel with the convex curvature, which tends to a rotation point further away from the wheel axis, presented the lowest capability to passively balance the system. The wheel with the concave curvature, which tends to have a rotation point closer to the wheel axis, presented the highest capability to passively balance the system.

Additionally, as the center of mass vertical position (CM_y) decreases, the robotic system tends to stabilize at lower values of angular displacement. For a CM_y located below the cross arm it is possible to passively stabilize the robotic system for every rotation point evaluated with an angular displacement below 20°, see Fig. 12.

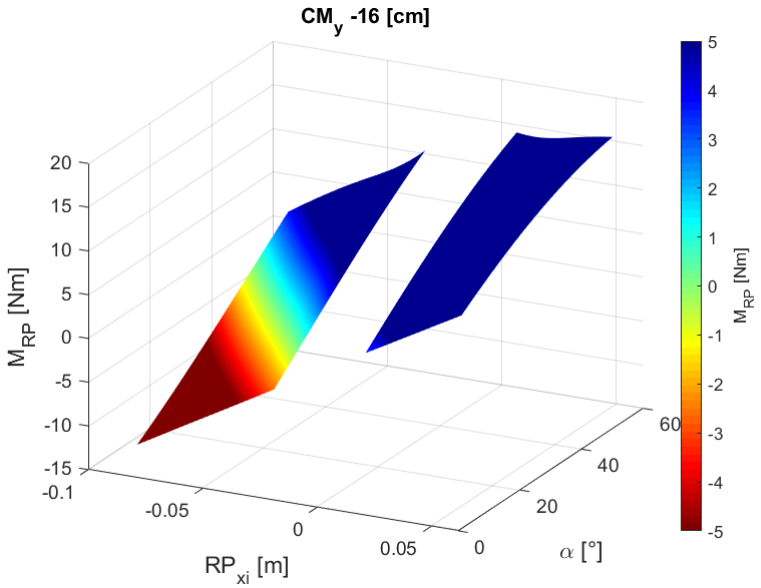

Figure 8: Output graph from the script.

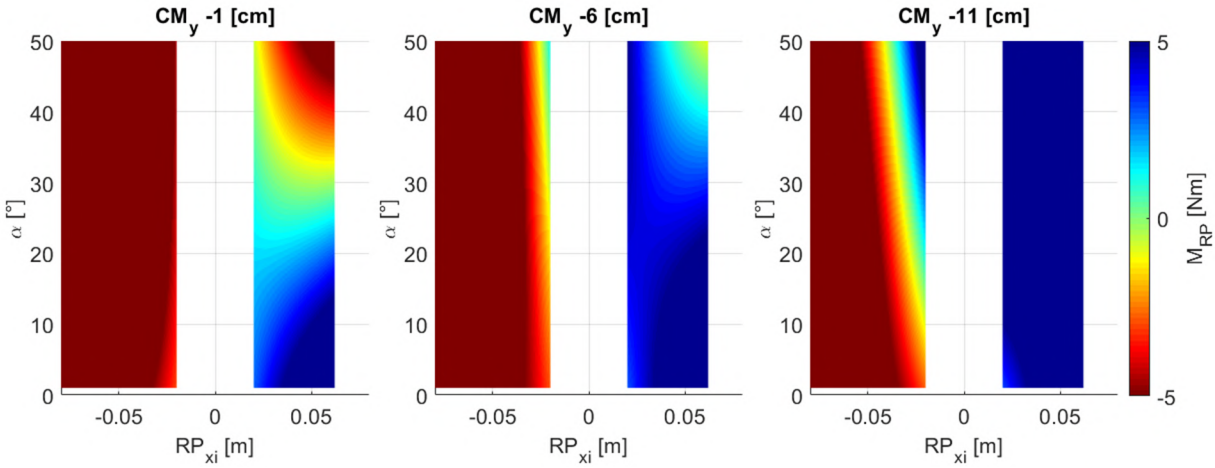

Figure 9: Output graphs for convex wheel curvature.

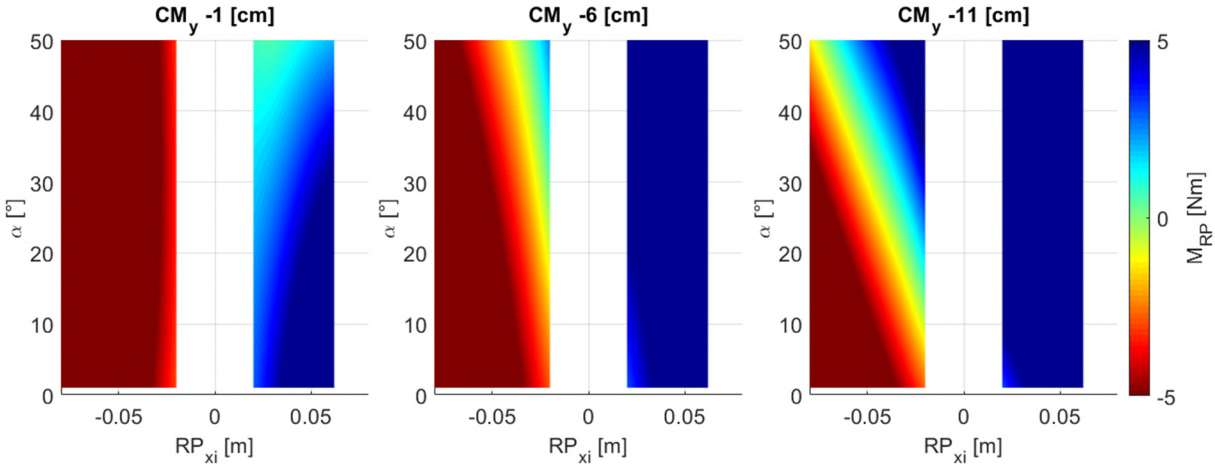

Figure 10: Output graphs for opposing concavities wheel curvature.

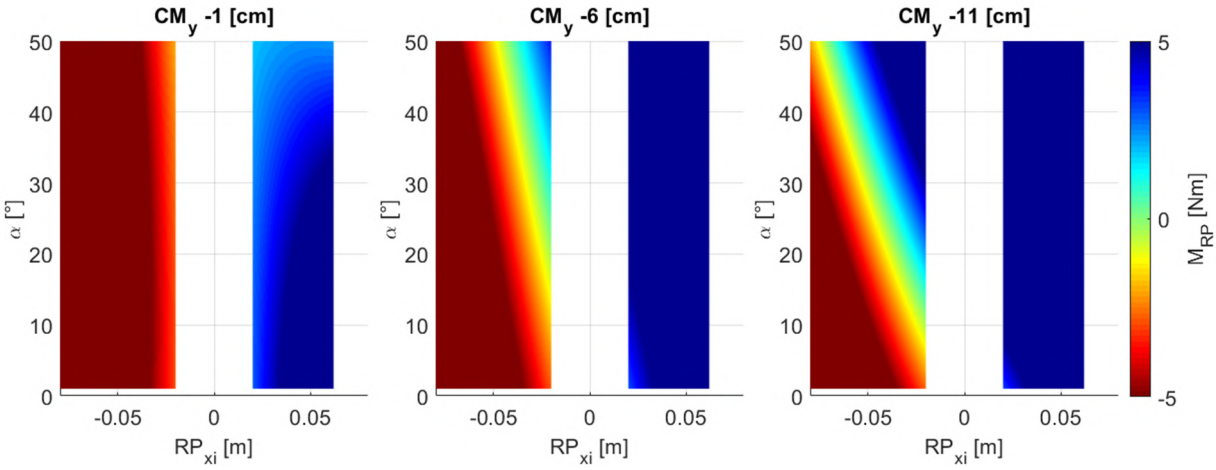

Figure 11: Output graphs for concave wheel curvature.

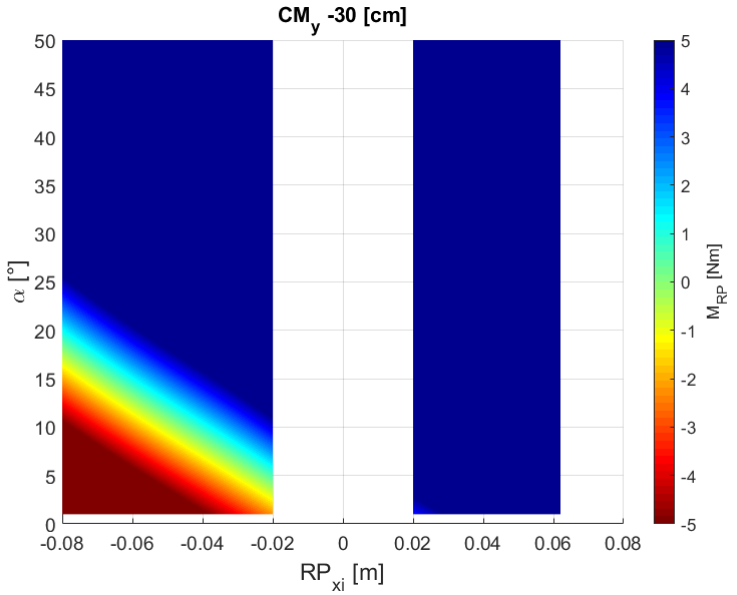

Figure 12: Output graph for center of mass located below the cross arm.

Overall, in this analysis the concave wheel curvature presented a slightly higher capability to passively balance the robotic system when compared to the wheel curvature with opposing concavities. However, when experimenting with prototypes, it was possible to observe that the wheel curvature with opposing concavities presented a better dynamic response to the obstacles, specially to center the wheel back to the conductor as the robot comes down from the insulator.

6. CONCLUSIONS

This paper investigated the static equilibrium capability of three different wheel geometries (opposing concavities, convex and concave curvatures) of a robotic system that rolls over distribution lines obstacles. The geometries are analyzed in regard to the moment sum at the rotation point for different rotation points and angular displacements. The impact of the center of mass on the equilibrium capability is also assessed. Stability maps are produced for each wheel to make it easier to visualize the robot equilibrium capacity and to aid design team to make decisions on the robot wheel design.

In the results presented, it is seen that for all wheels considered, the robot equilibrium capability is reduced as the rotation point laterally distances from robot center. This occurs because the wheel geometries have higher radius at both of their extremities. So, once the rotation point moves out of the central region, it gets vertically closer to the robot center of mass, reducing the robot balancing capacity. Therefore, when lower center of masses are considered for all wheel geometries, the equilibrium capacity increases. On the other hand, the wheel radius variation is necessary in order to guarantee that the robot can retake its alignment with the aluminium conductor after the robot passes through any distribution line obstacle.

For the same center of mass position, the wheel that yields higher balancing capability (smaller red areas in Fig. 9,

10 and 11) is the concave geometry wheel. However, the opposing concavities geometry presented stability maps that are relatively similar to the concave profile. At the same time, the opposing concavities wheel has a convex arc at its center that contributes to centralize the robot at the cable after the robot comes down from the insulator. Therefore, the design team chose the opposing concavities geometry for the robotic system being developed.

Future works include the investigation of optimum radii for the convex and concave geometries. Also, depending on the robot velocity, the impact onto obstacles may cause the robot to oscillate, to detach from the line or to jump over the obstacle. To delve into the analysis, a second study will be carried out to take the robot dynamic behaviour into account. The authors will analyze the robot performance experimentally, validating the robot dynamic behaviour under external disturbances and when transposing complex obstacles geometries.

7. ACKNOWLEDGEMENTS

This work was made as part of the R&D project entitled ”Development of a Robotized System for Inspection of Electricity Distribution Lines” (05697-0317 / 2017), regulated by ANEEL and financed by Centrais Elétricas de Santa Catarina (Celesc). The project is executed at the Laboratory of Applied Robotics (LAR), at UFSC, and financially managed by FEESC. The authors also thank CNPq and CAPES for the financial support.

8. REFERENCES

Aracil, R., Ferre, M., Hernando, M. and Sebastian, J.M., 2002. “Telerobotic system for live-power line maintenance: Robtet”. *Control Engineering Practice*, Vol. 10, No. 11, pp. 1271–1281.

Celesc, 2014. “E-313.0002: Estruturas para redes aéreas convêncionais de distribuição”.

Celesc, 2015. “E-313.0018: Cabo de alumÍnio nu - ca e caa”.

Fan, C., Li, E., Yang, G., Deng, H., Tan, M., Huang, S., Zhao, X., Hou, Z. and Liang, Z., 2011. “Two-arm swing obstacle-clearing type line walking robot body”. CN101752804B.

Gonçalves, R.S. and Carvalho, J.C.M., 2014. “A mobile robot to be applied in high-voltage power lines”. *Journal of the Brazilian Society of Mechanical Sciences and Engineering*, Vol. 37, pp. 349–359. doi:10.1007/s40430-014-0152-0.

Hibbeler, R., 2017. *Estática: mecânica para engenharia*. Pearson Education do Brasil. ISBN 9788543016245.

Hydro-Québec, 2018. “Lineranger: A revolution in transmission line robotics”. Hydro-Québec, http://www.hydroquebec.com/robots/en/. Accessed 28 August 2018.

IEEE, 2010. “Expliner”. IEEE, ROBOTS your guide to the world of robotics, https://robots.ieee.org/robots/expliner/. Accessed 16 June 2021.

Jalal, M.F.A., Sahari, K., Anuar, A., Arshad, A.D.M. and Idris, M.S., 2013. “Conceptual design for transmission line inspection robot”. Earth and Environmental Science.

Jenssen, R., Roverso, D. *et al.*, 2018. “Automatic autonomous vision-based power line inspection: A review of current status and the potential role of deep learning”. *International Journal of Electrical Power & Energy Systems*, Vol. 99, pp. 107–120.

Katrasnik, J., Pernus, F. and Likar, B., 2010. “A survey of mobile robots for distribution power line inspection”. *IEEE Transactions on Power Delivery*, Vol. 25, No. 1, pp. 485–493.

Miller, R., Abbasi, F. and Mohammadpour, J., 2017. “Power line robotic device for overhead line inspection and maintenance”. *Industrial Robot*, Vol. 44, No. 1, pp. 75–84.

Parker, L.E. and Draper, J.V., 1998. “Robotics applications in maintenance and repair”. *Handbook of industrial robotics*, Vol. 2, pp. 1023–1036.

Prates, R.M., Cruz, R., Marotta, A.P., Ramos, R.P., Simas Filho, E.F. and Cardoso, J.S., 2019. “Insulator visual non-conformity detection in overhead power distribution lines using deep learning”. *Computers & Electrical Engineering*, Vol. 78, pp. 343–355.

Rodmilans, G.B., Dos Santos, M.S., Da Silva, P.B. and Cunha, V.J.G., 2010. “Dispositivo robótico para superação de obstáculos em inspeção de linhas de transmissão de alta tensão”. PI1005861-3 A2.

Toussaint, K., Pouliot, N. and Montambault, S., 2009. “Transmission line maintenance robots capable of crossing obstacles: state-of-the-art review and challenges ahead”. *Journal of Field Robotics*, Vol. 26, No. 5, pp. 477–499.

Wang, L., Liu, F., Xu, S., Wang, Z., Cheng, S. and Zhang, J., 2010. “Design, modeling and control of a biped line-walking robot”. *International Journal of Advanced Robotic Systems*, Vol. 7, No. 4, p. 33. doi:10.5772/10498. URL `https://doi.org/10.5772/10498`.

Zongyuan, M., Lianfang, T. and Xiaohong, W., 2010. “Three-wheel inspection robot mechanism capable of crossing over catenary of pole and tower”. CN101859989B.

9. RESPONSIBILITY NOTICE

The authors are solely responsible for the printed material included in this paper.